

Interaction of Phenothiazine Compounds with Zwitterionic Lysophosphatidylcholine Micelles: Small Angle X-ray Scattering, Electronic Absorption Spectroscopy, and Theoretical Calculations

Leandro R. S. Barbosa, Wilker Caetano, and Rosangela Itri*

Instituto de Física, Universidade de São Paulo, Cx. Postal 66318, CEP 05315–970, São Paulo, SP, Brazil

Paula Homem-de-Mello, Patrícia S. Santiago, and Marcel Tabak

Instituto de Química de São Carlos, Universidade de São Paulo, Cx. Postal 780, CEP 13560–970, São Carlos, SP, Brazil

Received: November 9, 2005; In Final Form: March 28, 2006

In this work, small-angle X-ray scattering (SAXS) studies on the interaction of the phenothiazine cationic compounds trifluoperazine (TFP, 2–10 mM) and chlorpromazine (CPZ, 2–10 mM) with micelles of the zwitterionic surfactant L- α -lysophosphatidylcholine (LPC, 30 mM), at pHs 4.0 and 7.0, are reported. The SAXS results demonstrate that, upon addition of both phenothiazines, the LPC micelle of prolate ellipsoidal shape changes into a cylindrically shaped micelle, increasing its axial ratio from 1.6 ± 0.1 (in the absence of drug) to 2.5 ± 0.1 (for 5 and 10 mM of phenothiazine). Such an effect is accompanied by a shrinking of the paraffinic shortest semiaxis from 22.5 ± 0.3 to 20.0 ± 0.5 Å. Besides, a significant increase in polar shell electron density from 0.39(1) to 0.45(1) e/Å³ is observed, consistent with cylinder-like aggregate geometry. Moreover, an increase of the phenothiazine concentration induces the appearance of a repulsive interference function over the SAXS curve of zwitterionic micelles, which is typical of interaction between surface-charged micelles. Such a finding provides evidence that the positively charged phenothiazine molecule must be accommodated near the hydrophobic/hydrophilic inner micellar interface in such a way that a net surface charge is altered with respect to the original overall neutral zwitterionic micelle. Such phenothiazine location is favored by both electrostatic and hydrophobic contributions, giving rise to binding constant values, obtained from electronic absorption results, that are quite larger compared to their binding to another zwitterionic surfactant, 3-(*N*-hexadecyl-*N,N*-dimethylammonio)propanesulfonate (HPS) (Caetano, W., et al. *J. Colloid Int. Sci.* **2003**, *260*, 414–422). Comparisons are made by means of theoretical calculations of the surfactant headgroup dipole moments for monomers of LPC and HPS. The theoretical results show that the dipole moment in LPC is almost perpendicular to the methylene chain, while a significant contribution along the methylene chain occurs for HPS. Besides, evidence is presented for extensive delocalization of the charges in the headgroups, which could be also relevant for the binding of the drugs.

Introduction

Phenothiazine compounds are commonly used in clinical medicine as antipsychotic and tranquilizer drugs.^{1–4} They have interesting physicochemical properties associated both with their capacity to self-aggregate, forming “micelle-like” structures, as well as to change the properties of natural and model biomembranes.^{5–11} Despite a considerable amount of research dealing with the effects of such drugs upon membranes, both natural and model ones, the detailed interaction mechanism of these compounds with biomembranes is not well understood at the molecular level yet.

The interaction of two cationic phenothiazine derivatives, chlorpromazine (CPZ) and trifluoperazine (TFP) (Figure 1), with ionic micelles has been previously monitored through electronic absorption and fluorescence spectroscopies.^{12,13} The apparent pK_a changes of the drugs induced by the micelles were observed to be consistent with a strong interaction. The binding constants (K_b) showed a significant hydrophobic contribution modulated

by electrostatic interactions of the positively charged drug with the micelle headgroup. The special characteristics of the drugs binding to anionic sodium dodecyl sulfate (SDS) monomers and/or micellar aggregates were also focused.¹³ K_b values are higher than 5×10^3 M^{−1} for both SDS concentration ranges, at low surfactant concentrations and up to 1–2 mM (drug interaction with surfactant monomers and formation of nonmicellar aggregates) and for more concentrated solutions (in the presence of premicellar and/or micellar aggregates).

Subsequently, a small-angle X-ray scattering (SAXS) study was performed on the interaction of CPZ with SDS micelles.¹⁴ The results demonstrated that the shape and size of the drug/SDS mixed micelles are both SDS concentration and SDS:CPZ molar ratio dependent. Further, the SAXS data evidenced a micellar shape transformation from a small prolate ellipsoid with axial ratio $\nu = 1.5$ (for 40 mM SDS micelles in the absence of the drug) to a cylinder-like aggregate of $\nu = 2.5$ (with addition of 10 mM CPZ). Such micellar growth is triggered by a surface charge screening as the molar ratio drug:surfactant increases in the complex. Further, the influence of TFP on the micellar

* Corresponding author. Phone: (55) (11) 3091-7012. Fax: (55) (11) 3091-6749. E-mail: itri@if.usp.br.

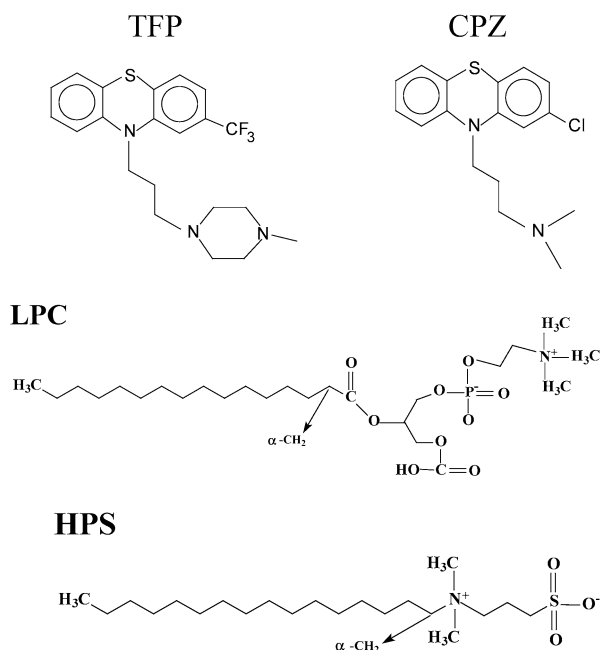


Figure 1. Schematic drawing of the chemical structures of the phenothiazine compounds CPZ and TFP and of the surfactants LPC and HPS used in this work.

properties of SDS (40 mM) as well as on the zwitterionic 3-(*N*-hexadecyl-*N,N*-dimethylammonio)propanesulfonate (HPS, 30 mM) micelles was also investigated by means of SAXS.¹⁵ The main difference related to the CPZ is that the TFP molecule possesses two pK_a values attributed mainly to the nitrogens of the hydrophobic piperazinic group attached to the phenothiazine ring ($pK_{a1} = 4.0$ and $pK_{a2} = 8.0$, for micromolar concentrations in aqueous solution³) in comparison to the unique nitrogen of the CPZ alkyl amino group attached to the phenothiazine heteroaromatic ring (Figure 1) (CPZ $pK_a = 9.3$, for micromolar concentrations in aqueous solution³). In the presence of SDS micelles the pK_a of CPZ increases to 10 while for HPS and neutral Brij-35 it has values of 8 and 7.8, respectively.¹² In the case of TFP in the presence of micelles, a unique pK_a of 4.4 is observed for SDS, 3.6 for HPS, and 2.7 for Brij-35.¹² The highest pK_a for TFP (8 in buffer) in the presence of surfactants was not observed, suggesting that the second deprotonation is not so easy in the presence of surfactants. In this way, CPZ is always monoprotonated at acidic and neutral pH, while at pH greater than 9 it is partially protonated to a greater or lesser extent, depending on the surfactant. In the case of TFP it must be always monoprotonated at neutral and basic pH and appears to be partially diprotonated at pH below 4.

An additional interest concerning the study of the structural effects of TFP upon the surfactant aggregates and in comparison to CPZ effects is associated with the fact that it is one of the most efficient compounds in this class both regarding the antipsychotic effect² and the reversal of multidrug resistance (anti-MDR effect) in connection with its coactivator activity of antitumor drugs.⁴

The aim of the present work is to further investigate the interaction of these kinds of drugs with micelles of distinct headgroup nature. Measurements are now focused on the interaction of CPZ and TFP with zwitterionic L- α -lysophosphatidylcholine (LPC) in comparison to the drug assembling with zwitterionic HPS micelles.¹⁵ We are going to demonstrate that the binding of this sort of positively charged drugs to LPC is significantly higher than to HPS. Figure 1 includes a scheme of the chemical structures of both LPC and HPS molecules.

Interestingly, one could think that the LPC micelles may have the charges that form the dipole at the interface located in such a way that the opposite orientation as compared to HPS would be expected (Figure 1). Nevertheless, theoretical calculations of the conformations of LPC and HPS monomers will be also shown and suggest significant differences in the dipole orientation for both surfactants, but they are not opposite as appears from the simplified scheme of Figure 1. Comparisons will be also made with respect to the features of interaction between anionic porphyrins, which are negatively charged compounds, to HPS.¹⁶ We expect to obtain further insights on the interactions of drug-micelles from our present studies.

2. Materials and Methods

2.1. Materials. Trifluoperazine dihydrochloride (TFP, Sigma Chemical Co.), chlorpromazine hydrochloride (CPZ, Sigma Chemical Co.), L- α -lysophosphatidylcholine (LPC, Sigma Chem. Co.), sodium acetate, and monobasic sodium phosphate (Mallinckrodt) were used as purchased. Ultrapure Milli-Q (18.2 M Ω /cm) water was employed. The pH values were adjusted with calibrated solutions of HCl and NaOH and measured by means of either a Corning-130 or a Digimed pH-meter.

The sample preparation using a surfactant stock solution of 0.2 M LPC followed the same protocol as described in ref 15.

2.2. Binding Constant Determination (K_b). The binding of the phenothiazines to LPC monomers and/or micelles was investigated by means of electronic absorption spectroscopy using the red shifts of the maximum absorption upon titration of a phenothiazine solution of fixed concentration with increasing concentrations of surfactant. The titration of the drugs in solution as a function of LPC concentration makes it possible to evaluate association constants of CPZ or TFP to LPC during an equilibrium process in solution. The titrations and the spectra acquisition were performed on a Hitachi U-2000 spectrophotometer coupled to an IBM computer. For each titration at chosen pHs, wavelengths were selected to perform the experiment with the maximum sensitivity. The drug samples had the concentration 5×10^{-5} M in 2 mL of 20 mM acetate buffer at acidic pH 4.0 or 20 mM phosphate buffer at neutral pH 7.0. The titration was performed by successive additions of small aliquots of a surfactant stock solution directly into a 1 cm optical absorption quartz cuvette. Corrections were made in the measured absorbance due to dilution caused by addition of surfactant aliquots during titration. Further details on determination of association constants are described in refs 12 and 13.

2.3. Small Angle X-ray Scattering. SAXS experiments were performed at National Laboratory of Synchrotron Light (LNLS, Campinas, Brazil) at room temperature (22 ± 1 °C), with radiation wavelength $\lambda = 1.608$ Å and sample-to-detector distance of ~ 744 mm. Micellar aqueous solutions of 30 mM LPC in the absence and presence of increasing drug concentration (0, 5, and 10 mM), were prepared in 20 mM of sodium acetate and phosphate at pH 4.0 and 7.0, respectively. Accordingly, the drug:LPC molar ratio (M_{drug}) were 0, 0.17, and 0.33. Samples were set between two mica windows and a 1 mm spacer, handled in a liquid sample-holder. This was placed perpendicular to the primary X-ray beam. The obtained curves (data collection of 15 min) were corrected for detector homogeneity (one-dimension position sensitive detector) and normalized by taking into account the decrease of the X-ray beam intensity during the experiment. The parasitic background (buffer solution) was subtracted considering the sample's attenuation. Two sets of measurements were taken from each sample after a time interval of 2–4 h, showing reproducible scattering data.

The final spectra correspond to an average of the corrected data for each studied sample.

It is well-known that the SAXS intensity $I(q)$ of an isotropic solution of monodisperse spheroidal particles of low anisotropy (smaller than 3) can be described as¹⁷

$$I(q) = kn_p P(q) S(q) \quad (1)$$

where n_p corresponds to the particle number density and k is a normalization factor related to the instrumental effects ($q = 4\pi \sin \theta/\lambda$ is the scattering vector; 2θ is the scattering angle). $S(q)$ corresponds to the interparticle interference function that tends to 1 for noninteracting particles. This is the case for low concentrated dispersions of zwitterionic micelles that act as neutral aggregates.¹⁵ Nevertheless, as will be shown below, the incorporation of the cationic phenothiazine molecules into LPC micelles leads to the appearance of an interference function over the SAXS curves in a similar way as occurs for ionic micelles dispersed in an aqueous solution of low ionic strength.^{14,15,18} Then, in the current work, $S(q)$ is calculated by means of Hayter and Penfold's methodology,^{19,20} which associates the micelles as charged spheres interacting through a screened Coulomb potential in the mean spherical approximation (MSA). The parameter $\alpha = z/n$, where z = net charge and n = mean aggregation number, accounts for the micellar surface charge.¹⁸

$P(q)$ in eq 1 is the orientational average of the particle form factor. In our case, the micelle will be modeled as a prolate ellipsoid²¹ and/or a cylinder.¹⁴ For both micellar shapes the shortest semiaxis is on the order of the paraffinic chain length, R_{par} (free parameter), whereas the largest semiaxis is νR_{par} , with ν equal to the axial ratio, another free parameter. The model assumes that the micelle is constituted by two shells of different electron densities: an inner core of paraffinic moiety, with electron density $\rho_{\text{par}} = 0.275 \text{ e}/\text{\AA}^3$, and an external shell, surrounding the core, with a respective polar headgroup thickness σ that includes the hydration water and electron density ρ_{pol} (free parameters) relative to the continuous medium (buffer solution with electron density assumed to be similar to that of the water $\rho_w = 0.327 \text{ e}/\text{\AA}^3$). The micellar form factor $P(q)$ and the effective sphere for $S(q)$ have an equal inner-hydrocarbon-core volume and are surrounded by a polar shell of thickness σ .^{14,18} The structural parameters and the micellar charge are then obtained by fitting the product $P(q) S(q)$ to the experimental curve, and k in eq 1 is a normalization factor that was kept constant for all samples.¹⁶

2.4. Theoretical Calculations. All calculations were performed using the semiempirical method PM3,²² as implemented in Gaussian 03 code. To reach the global minimum, some structural parameters of the initially optimized molecules were changed manually and the molecular structures were reoptimized. This procedure was repeated until no more change of structure was obtained. Afterward, the following properties were calculated for both surfactants: atomic charges by using Mulliken population analysis, dipole moments, headgroup volume (by solvent-accessible surface approximation, with solvent probe radius of 1.4 \AA), and paraffinic radius. The polar shell radius, R_{pol} , was obtained from headgroup volume under approximation to a sphere. Calculated atomic charges of several atoms are combined into submolecular groups that are expected to be meaningful to the physical properties of surfactants.^{23,24}

The optimized structures of LPC and HPS are shown in Figure 2, whereas the obtained structural data are displayed in Table 1.

2.5. Hydration in the Polar Shell. From ν , R_{par} , σ , and ρ_{pol} values extracted from the $P(q)$ fitting to the SAXS curves, one

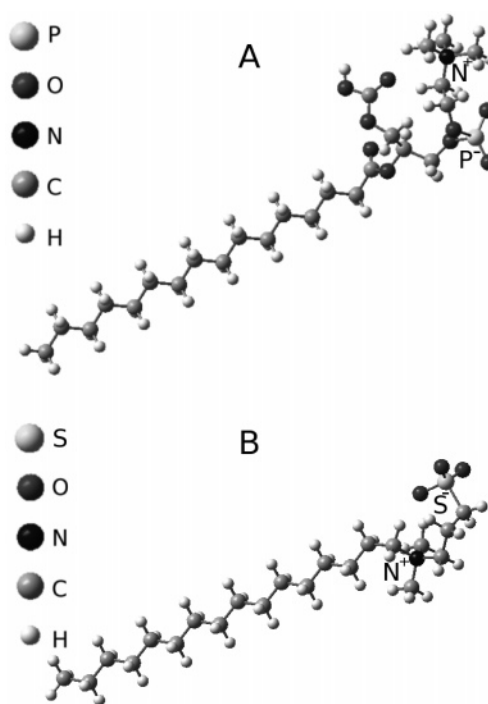


Figure 2. Structures of LPC (A) and HPS (B) obtained from PM3 geometry optimization.

can calculate the hydration number W_n in the polar shell, since ρ_{pol} is given by

$$\rho_{\text{pol}} = \frac{n_{\text{LPC}} n_e(\text{headgroup}) + n_{\text{drug}} n_e(\text{drug}) + W_n n_e(\text{H}_2\text{O})}{V_{\text{pol}}} \quad (2)$$

where n_{LPC} and n_{drug} correspond to the monomers number of LPC and drug in the micelle, respectively; $n = n_{\text{LPC}} + n_{\text{drug}} = n_{\text{LPC}}(1 + M_{\text{drug}})$. V_{pol} is the polar shell volume calculated from the σ value. $n_e(\text{H}_2\text{O}) = 10$ is the number of electrons of water molecule, and $n_e(\text{headgroup})$ and $n_e(\text{drug})$ are, respectively, the number of electrons of surfactant headgroup and of drug. These values will be inferred into the Discussion later in the text.

The mean aggregation number n of LPC/drug micelle can be calculated according to

$$n\nu_{\text{par}} = 4\pi\nu(R_{\text{par}})^3/3 \quad \text{for prolate ellipsoid} \quad (3a)$$

$$n\nu_{\text{par}} = 2\pi\nu(R_{\text{par}})^3 \quad \text{for cylinder-like micelle} \quad (3b)$$

where $n\nu_{\text{par}}$ is the volume of the inner hydrophobic portion of the micelle. If one assumes that, in the first approximation, $\nu_{\text{par}} = 459 \text{ \AA}^3$, corresponding to the 16C-alkyl chain volume²⁵ of the LPC molecule, including the carbon of the carbonyl group (Figures 1 and 2), n is easily determined from eq 3.

3. Results

Figure 3a shows, as an example, the electronic absorption spectra for TFP at LPC concentrations used in the titration procedure at pH 7.0. A red-shift of the maximum absorption is noted for drug-containing micellar solutions (LPC critical micellar concentration is around 0.2 mM). A similar result was observed for CPZ (data not shown). Figure 3b presents the corresponding fitting (eq 2 in ref 12) to the TFP titration experimental data, which allows us to determine the association constants K_b . Table 2 reports on LPC K_b values at pH 2.0, 5.0, and 7.0 for TFP and CPZ. A perusal of the data shows that the

TABLE 1: Parameters Obtained from PM3 Geometry Optimization of LPC and HPS Monomers^a

HPS		LPC ^b	
R_{par} (Å)	18.87	R_{par} (Å)	18.82(17.56)
R_{pol} (Å)	4.96	R_{pol} (Å)	5.68(5.85)
V_{pol} (Å ³)	512.3	V_{pol} (Å ³)	766.6(839.1)
charge on headgroup	-0.11	charge on headgroup	-0.05(-0.10)
charge on α -CH ₂	0.02	charge on α -CH ₂	0.09
charge on alkyl chain	0.09	charge on alkyl chain	0.02
charge on N(CH ₃) ₂	0.70	charge on N(CH ₃) ₃	0.78
charge on C ₃ H ₆	-0.41	charge on C ₂ H ₄	0.23
charge on SO ₃	-0.40	charge on PO ₄ ⁻	-1.11
dihedral angle N-C-C-C	-84.3	charge on CH(CH ₂) ₂	0.42
		charge on COO	-0.28
		charge on OCOOH	-0.15
		angle C _{alkyl} -C _{α} -C _{head} (deg)	110.4
		dihedral angle O-C-C-O (deg)	108.8
		angle O-P-O (deg)	96.0

^a Grouped atomic charges for selected groups. All distances were calculated from atomic coordinates. R_{pol} was calculated from V_{pol} assuming approximate spherical geometry for the headgroups. ^b Values in parentheses correspond to the carbonyl group also considered as part of the headgroup.

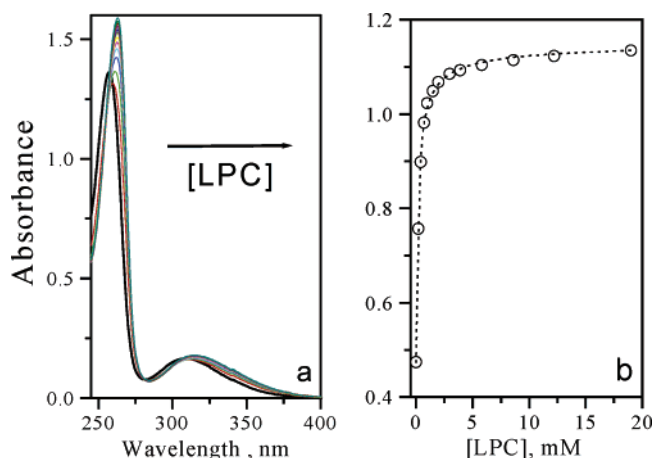


Figure 3. (a) Optical absorption spectra of TFP (5×10^{-5} M) in 20 mM acetate buffer at different LPC concentrations used in the titration at pH 7.0. Detergent concentrations are 0, 0.2, 0.4, 0.7, 1.0, 1.5, 2.0, 3.0, 3.9, 5.8, 8.6, 12.2, and 19 mM. (b) The symbols represent the absorbance at 268 nm extracted from the experimental data, and the dashed line is the result of the fitting to eq 2 in ref 12.

TABLE 2: Binding Constants (K_b) of TFP and CPZ (5×10^{-5} M) to LPC as a Function of pH Determined by Spectrophotometric Titration^a

pH (± 0.2)	binding constant, K_b (M ⁻¹)			
	TFP		CPZ	
	LPC	HPS	LPC	HPS
2.0	2163 \pm 60	707	2116 \pm 54	457
5.0	4145 \pm 150	1055	3361 \pm 53	480
7.0	4189 \pm 63	2247	3319 \pm 57	668

^a K_b values for HPS were taken from ref 12.

binding constants are higher for TFP as compared to CPZ at pHs 4.0 and 7.0 (Table 2), being smaller at pH 2.0 for both phenothiazine compounds. It seems that the high proton concentration in the bulk ($\sim 10^{-2}$ M) decreases the affinity of the cationic drugs for the micellar interface. The magnitude of this effect was clearly observed in studies of the interaction of TFP and CPZ with neutral micelles of the surfactant Brij-35 at pH 2.0, where a high proton density surrounding the long polyoxyethylene headgroup was assumed to be responsible for the significant decrease of the cationic drug binding.¹² A similar effect was also noted for the binding of these phenothiazine molecules to cationic cetyltrimethylammonium chloride (CTAC) micelles.¹²

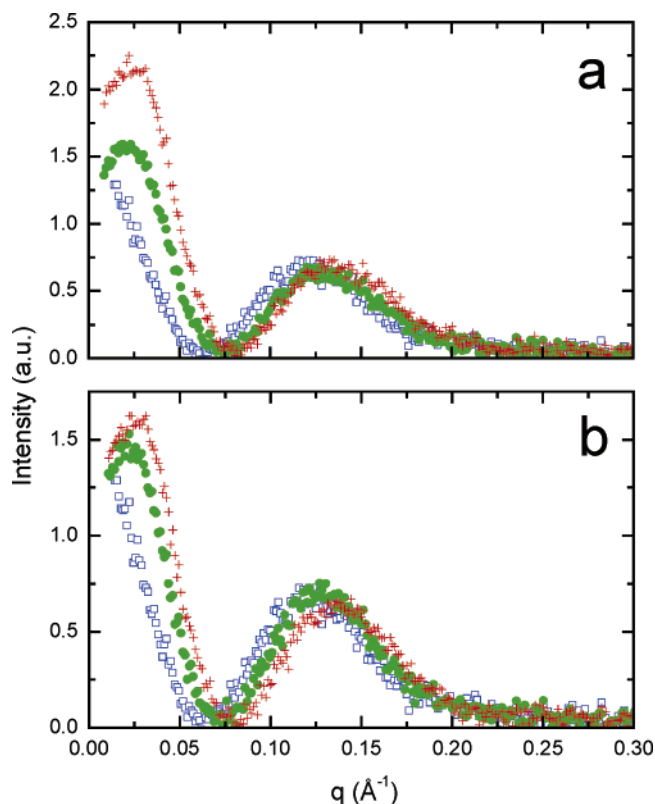


Figure 4. SAXS curves of 30 mM LPC in aqueous solution at pH 4.0, in absence of drug (blue color) and in the presence of increasing drug concentrations of 5 mM (green color) and 10 mM (red color): (a) TFP and (b) CPZ.

To elucidate the possible drug location and structural changes induced by the binding of positively charged drugs to zwitterionic model membranes at pHs 4.0 and 7.0, SAXS experiments were performed on LPC micelles in the absence and presence of TFP and CPZ. Figure 4 shows the SAXS data obtained from samples composed of 30 mM LPC under the influence of TFP (Figure 4a) and CPZ (Figure 4b), at pH 4.0, for increasing drug concentration up to 10 mM (up to $M_{\text{drug}} = 0.33$). As one can observe, the SAXS curves of drug-free micelles present a broad peak at $q \approx 0.12 \text{ Å}^{-1}$ characteristic of the intramolecular form factor,¹⁸ identical to that observed for HPS micelles.^{15,16,26} Such a peak moves toward longer q values upon both CPZ and TFP addition, giving the first evidence that the LPC micellar hydrophobic core is affected by drug incorporation, as will be shown by SAXS data analysis below.

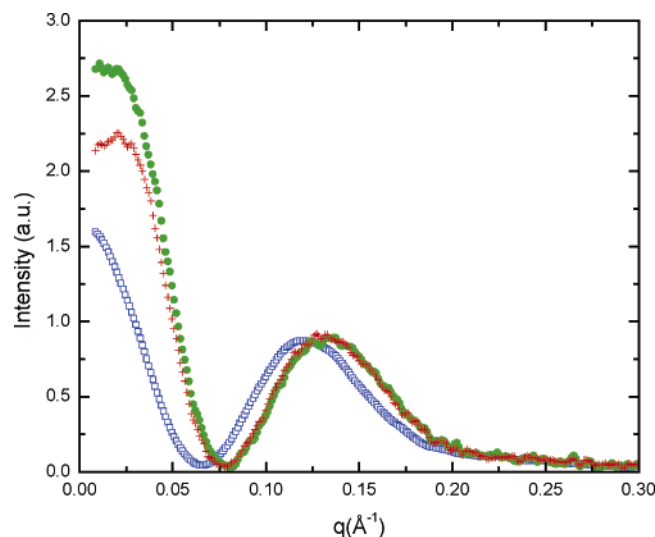


Figure 5. SAXS curves of 30 mM LPC in aqueous solution at pH 7.0, in absence of drug (blue color) and in the presence of 10 mM TFP (green color) and 10 mM CPZ (red color).

Furthermore, the presence of an inner peak ($q \approx 0.025 \text{ \AA}^{-1}$) for phenothiazine-containing LPC micelles is a fingerprint of an intermicellar interference function associated with the interaction of surface-charged micelles.^{14,15,18} Such a finding is remarkable and quite unexpected, since zwitterionic surfactants have a net charge on the headgroup close to zero (Table 1), unlike the ionic surfactants.²³ It means that the cationic drug must be interacting with LPC micelle in such a way that the mixed aggregate has a non-null overall charge at the micellar outer region.

The same features are observed at pH 7.0, as shown in Figure 5, upon binding of 10 mM of either CPZ or TFP to LPC micelles. Both drugs similarly affect the micellar shape, as revealed by the same intramicellar peak displacement to longer q values. Besides, an interference function also appears on the scattering curves, although to a different extent upon TFP versus CPZ incorporation.

With a view to better explore the features of the drug:LPC aggregates with respect to those observed for drug-free LPC micelles, the data were analyzed through modeling the intramicellar ($P(q)$) and intermicellar ($S(q)$) functions (eq 1), as follows. Figures 6 and 7 present the best fittings (thick lines) obtained from the samples at pH 4.0 and 7.0, respectively. Table 3 displays the corresponding fitting parameters.

The SAXS curves for pure LPC micelles are fitted by considering $S(q) = 1$ in eq 1, consistent with nonelectrostatic interaction between plain zwitterionic micelles. The results demonstrate that the micellar aggregates are well-represented by small prolate ellipsoids with axial ratio $\nu = 1.6 \pm 0.1$ and paraffinic radius R_{par} (the shortest axis) of $22.5 \pm 0.3 \text{ \AA}$ (Table 3), at acidic and neutral pHs (Figures 6 and 7), like the data obtained for drug-free HPS micelles.^{15,16,26} Such an R_{par} value, although 20% larger than that predicted from the geometry optimization of the molecule (Table 1), agrees with the extended length of the hexadecyl (21.8 Å) and heptadecyl (23.0 Å) chain according to Tanford's formula.²⁵ This reveals that the interface between the inner core and the headgroup region must reside between the α -methylene and the $\text{N}(\text{CH}_3)_2$ groups in the case of HPS micelle (Figures 1 and 2). For LPC, the interface must lie in the carbonyl group (COO, Figures 1 and 2). Noteworthy, even though both surfactants have a quite different polar head structure (Figure 2), the micellar aggregates self-assemble as small prolate ellipsoids, indicating that the spontaneous molec-

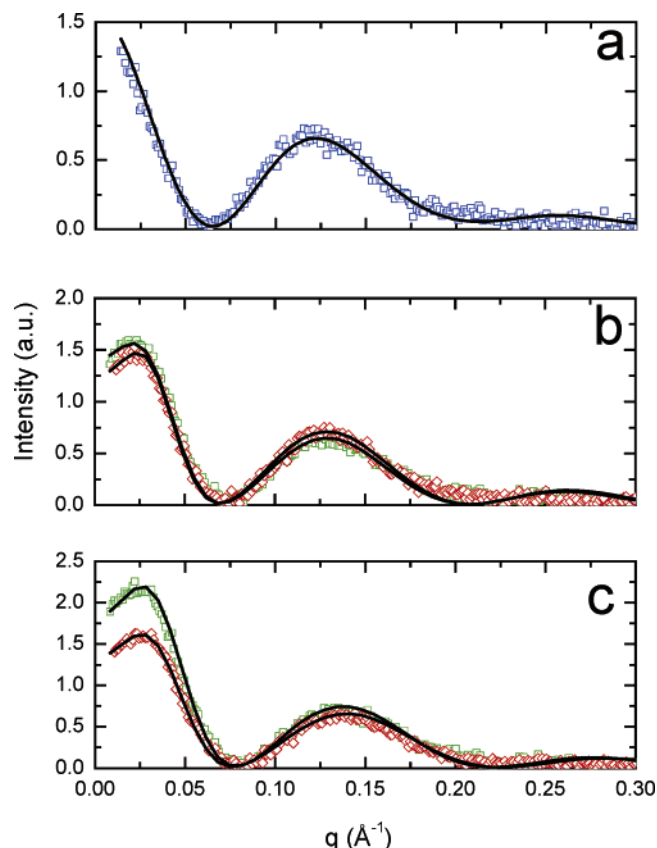


Figure 6. SAXS curves for 30 mM LPC at pH 4.0 in absence of drug (a) and in the presence of 5 mM (b) and 10 mM (c) of TFP (green color) and CPZ (red color). The thick lines represent the theoretical modeling (eq 1) in comparison to the experimental data. The fitting parameters are described in Table 3.

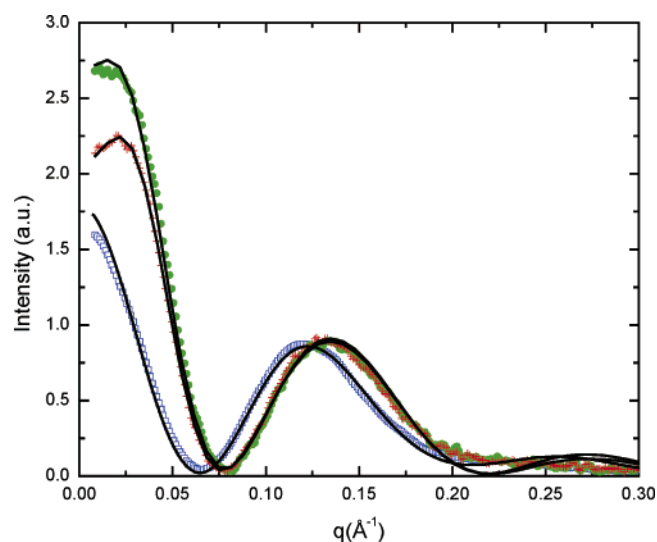


Figure 7. SAXS curves for 30 mM LPC at pH 7.0, in the absence of drug (blue color) and in the presence of 10 mM TFP (green color) and 10 mM CPZ (red color). The thick lines represent the theoretical modeling (eq 1) in comparison to the experimental data. The fitting parameters are described in Table 3.

ular surfactant parameter p_o , introduced by Israelachvili et al.,²⁷ must be alike for HPS and LPC [$p_o = \nu/al$, where ν , l , and a respectively are the hydrophobic chain volume, the effective chain length, and the polar head area (the area available per hydrophilic group at the hydrocarbon/water interface)].

Concerning the micellar features upon phenothiazine addition, we have found that the SAXS curves are better fitted by

TABLE 3: Values of Fitting Parameters Obtained from the Scattering Curves of Samples Composed of 30 mM LPC in the Absence and Presence of Increasing Drug Concentration at pHs 4.0 and 7.0^a

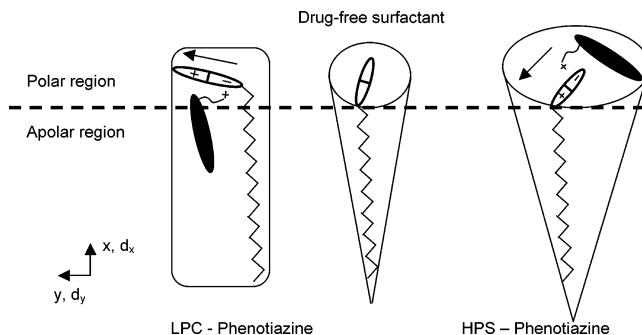
[drug] (mM)	pH	α	R_{par} (Å)	σ_{pol} (Å)	ρ_{pol} (e/Å ³)	ν	micellar shape
0	4.0 or 7.0	0	22.5(3)	9.0(2)	0.39(1)	1.6(1)	ellipsoid
Trifluoperazine (TFP)							
5	4.0	0.038(2)	22.0(5)	8.0(5)	0.45(1)	2.5(1)	cylinder
10	4.0	0.040(2)	20.0(2)	8.8(2)	0.44(1)	2.5(1)	cylinder
10	7.0	0.033(3)	21.0(5)	8.3(4)	0.45(1)	2.4(1)	cylinder
Chlorpromazine (CPZ)							
5	4.0	0.040(2)	22.0(5)	7.5(6)	0.45(1)	2.5(1)	cylinder
10	4.0	0.045(2)	20.0(5)	8.5(2)	0.44(1)	2.5(1)	cylinder
10	7.0	0.044(2)	21.0(5)	8.5(3)	0.44(1)	2.5(1)	cylinder

^a Legend: α = ionization coefficient, R_{par} = shortest paraffinic axis, σ_{pol} = polar shell thickness, ρ_{pol} = polar shell electron density, ν = axial ratio between the largest and the shortest paraffinic axis. The uncertainties are represented in parentheses.

cylinder-like aggregates than by ellipsoids as both CPZ and TFP are added to LPC micelles, whatever the drug concentration. Such micelle shape transformation is accompanied by micellar growth. In fact, the micellar axial ratio increases from 1.6 (drug-free micelle) to $\nu = 2.5 \pm 0.1$ at pHs 4.0 and 7.0. Furthermore, the intramicellar peak displacement is associated with a reduction of the shortest paraffinic axis to $R_{\text{par}} = 20.5 \pm 1.0$ Å (shrinking of ca. 10%) without any significant change in the polar head thickness $\sigma \approx 9$ Å at both pHs. Concurrently, the polar shell electron density increases from $\rho_{\text{pol}} = 0.39 \text{ e/Å}^3$ for ellipsoidal micelles in the absence of drugs to $\rho_{\text{pol}} = 0.45 \text{ e/Å}^3$ for drug-containing LPC micelles of cylindrical shape. This is easily understood once the available volume per polar head is greater for spheroids than for cylinders. Another interesting point is related to the fact that the drug binding to the zwitterionic LPC micelles induces the appearance of an interference function over the SAXS curves (Figures 6 and 7). Indeed, the fitting results reveal that, although the ionization coefficient α is small (Table 3), there is a significant repulsive interaction between the mixed aggregates. For instance, taking into account the values of $\nu = 2.5$, $R_{\text{par}} = 20.0$ Å, and $\alpha = 0.04$ extracted from the fitting procedure (Table 3), a mean aggregation number $n = 274$ (eq 3) is found for the cylinder-like aggregate at pH 4.0, upon the addition of 10 mM drug ($M_{\text{drug}} = 0.33$, corresponding to 90 drug molecules to 184 LPC molecules). Taken together, $n = 274$ and $\alpha = 0.04$, one can infer the number of charges in the micelle surface as $z = 11$. It should be remarked that z must be considered as an effective value, once α is a free parameter and it can suppress the deficiencies of the potential used in the analysis methodology.¹⁸

4. Discussion

The extent of binding of TFP (and CPZ) to LPC micelles is extracted from Figure 3 and presented in Table 2. The data evidence a higher binding constant of TFP as compared to CPZ at pHs 5.0 and 7.0, reinforcing a higher hydrophobic character for TFP.¹² In a previous investigation¹² we showed that the binding constants of CPZ to HPS micelles change only slightly (Table 2), consistent with the monoprotonated state of CPZ remaining constant in this pH range. Further, the association constants evaluated for TFP to HPS (Table 2) were greater than those found for CPZ, with a 3-fold increase on going to higher pH (from pH 2.0 to pH 7.0). Then, the importance of the TFP protonation state for HPS binding is clear. In the case of LPC studied here, the binding constants were quite higher for both

**Figure 8.** Scheme of the LPC and HPS micellar packing in the absence and presence of phenothiazine. The arrows represent the respective dipole moment directions relative to the reference axes x and y .

drugs in comparison to that of HPS (Table 2). Therefore, the distinct affinities observed for both drugs to HPS and LPC indicate that the micellar structure, in particular the possibility of inversion in dipole orientation of the zwitterion headgroup and/or the differences in headgroup charge distribution (Figures 1 and 2), could play an important role in the binding forces of these positively charged phenothiazine compounds to the studied zwitterionic micelles.

At this point, it is worthy considering the results of theoretical calculation regarding the geometry optimization for LPC and HPS monomers using the procedures described in the Materials and Methods section. Examination of the results in Table 1 shows that not all of the charges are concentrated in the ionic species existent in the headgroups, but a significant fraction of charge is distributed among various parts of the headgroup, the α -methylene group, and even the remaining alkyl tail (Figures 1 and 2). In LPC there is a significant negative charge associated with the phosphate group (-1.11), which lies in the border of the hydrophobic micelle core, while the positive charge is distributed among several groups. A fraction of positive charge appears in the alkyl tail (0.11 including the α -methylene), and the overall headgroup charge is negative if the carbonyl is not included in the headgroup (-0.05), remaining negative and increasing 2-fold if it is included (-0.10). In HPS, the negative charge is distributed between the sulfate (-0.40) and the nearby C_3H_6 (-0.41). The positive charge on the nitrogen (0.70) is also significantly distributed over the alkyl tail, where a positive charge of 0.11 (including the α -methylene) is obtained. The overall headgroup charge is also negative (-0.11), similar to that obtained for LPC.

Looking at the charge distribution, there is a negative charge site nearby the hydrophobic core of LPC (COO and OCOOH groups, Figure 2 and Table 1) that may favor the binding of positively charged drugs through electrostatic and hydrophobic driven forces. Unlikely, the charge distribution at the hydrophobic core interface of HPS micelle is highly positive ($\text{N}(\text{CH}_3)_2$ group). Then, although the drugs are hydrophobic and must be partially incorporated into the paraffinic region of the micelle, the positive charge at the inner interface must inhibit the binding of the cationic drugs due to the counterbalance of electrostatic forces of repulsive character.

Furthermore, the dipole moments were also calculated for both surfactants. In the case of HPS an overall dipole moment of 16.9 D was obtained, with components $d_x = -10.58 \text{ D}$, $d_y = 13.16 \text{ D}$, and $d_z = 0.63 \text{ D}$. For LPC, a total dipole moment of 13.95 D was obtained with components $d_x = 2.51 \text{ D}$, $d_y = 13.58 \text{ D}$, and $d_z = -1.98 \text{ D}$. The x -axis direction is along the methylene chain. The resulting \vec{p} vectors are schematically drawn in Figure 8. So, \vec{p} points toward the inner and outer region of the HPS and LPC micelle, respectively. However, it is worth

noting that the dipole moment in the plane yz is practically the same for both HPS and LPC molecules, differing significantly in the magnitude and sense in the x -axis direction. As a consequence, a positive charge (or a molecule carrying a positive charge) is driven away from the HPS micelle surface to the bulk solution. Conversely, a positive charge is attracted to the inner part of the LPC micelle, although the attractive dipole component along the x -direction must exert a smaller extent in LPC micelles than does the repulsive d_x component in HPS micelles. The LPC dipole moment here obtained is consistent with calculations for the dipole moment of dipalmitoyl phosphatidylcholine phospholipid, DPPC, for which a large dipole moment of around 10 D is obtained with an almost perpendicular orientation relative to the methylene double chain.^{28,29} Therefore, the charge distribution presented in Table 1 and the components of the dipole moments along the x -direction of these surfactants suggest that these physical parameters must play an important role in the interaction of the different drug molecules with these micelles. Noteworthy, even though the modulus of the LPC d_x component is weak as compared to the d_x modulus in HPS, the binding constants of the cationic TFP and CPZ molecules are significantly higher to LPC than to HPS.

The SAXS results presented in Table 3 demonstrate that the presence of the cationic phenothiazine compounds in LPC micelles leads to the formation of cylinder-like micellar aggregates of longer sizes with a slightly more packed hydrophobic core in comparison with the pure ellipsoidal LPC micelles. Furthermore, the positively charged phenothiazine molecules must be placed nearby the hydrophobic region and polar head interface, as schematically shown in Figure 8. Such drug location barely affects the polar shell thickness, but they induce a non-null overall surface micelle charge.

The CPZ and TFP location in the micelle must be driven by the surfactant electric dipole formed by positive and negative groups that must stabilize the orientation of the positive charges of the phenothiazines toward the negative ones of the zwitterions near the hydrophobic/hydrophilic interface (inner micellar interface) (Figure 8). This may enhance the binding of the protonated drug to the LPC micelle, because both electrostatic and hydrophobic contributions are favored in this situation. Studies concerning the interaction of another phenothiazine derivative, metachlorpromazine, with DPPC and DPPC/cholesterol liposomes by ^1H and ^{31}P RMN have shown a significant immobilization of the phosphate group in the choline moiety in the presence of the drug,³⁰ probably due to the strong interaction and location of the drug at the vesicle interface near the headgroup.

In terms of hydration of the polar shell, taking ν and R_{par} values into account, a mean aggregation number n of 166 (eq 3) is determined for both HPS and LPC micelles in the absence of drug. The only difference observed between the fitting parameters obtained from the micelles scattering curves of HPS^{15,16} and LPC micelles is related to the polar shell thickness ($\sigma = 7.4$ and 9.0 Å, respectively). Accordingly, a hydration number W_n of 11 water molecules per HPS monomer (eq 2) is found in the bipolar shell [by considering the $\text{N}(\text{CH}_3)_2$ group pertaining to the shell with $n_e(\text{HPS, headgroup}) = 89$ electrons], whereas $W_n = 9$ and 11 are determined for LPC with $n_e(\text{LPC, headgroup}) = 173$ and 151 electrons, respectively, considering that the carbonyl group makes part of the LPC micelle headgroup or not.

In the case of incorporation of a phenothiazine drug, CPZ for instance, into HPS micelles, our prior SAXS data¹⁶ revealed a small decrease in the micelle anisometry accompanied by

shrinking of the paraffinic radius ($R_{\text{par}} = 19.5$ Å, $\nu = 1.35$, $\sigma = 7$ Å, $\rho_{\text{pol}} = 0.40$ e/Å³). This results in a mean aggregation number $n = 91$ with 15 water molecules per HPS or CPZ monomers, under the condition that just the CPZ tail is in the polar shell [$n_e(\text{CPZ}) = 49$ electrons], or $W_n = 13$ for the whole CPZ molecule in the polar head [$n_e(\text{CPZ}) = 168$ electrons]. Making a parallel with LPC, the micelle underwent a shape transformation from spheroid to cylinder-like aggregate with $\nu = 2.5$ ($n = 274$), upon the CPZ binding at pH 4.0 (Table 3). Such geometry leads to a number of 9 and 5 water molecules per LPC or CPZ monomer in the case that the CPZ tail and the phenothiazine whole molecule are, respectively, considered part of the polar shell.

To conclude, the smaller K_b values found for TFP and CPZ binding to HPS with respect to LPC must be due to a significant contribution of the dipole moment of HPS as well as a significant positive charge delocalized to the alkyl chain and a negative charge delocalized in the polar shell precludes the positively charged drug binding near the inner micellar interface, as represented in Figure 8. Hence, the binding of an anionic drug to HPS must be favored. This was indeed recently demonstrated for the binding of anionic porphyrin molecules to HPS,¹⁶ where the K_b values are at least 1 order of magnitude higher than those of TFP (and CPZ) to HPS.¹² Besides, similarly to the data presented here, the respective SAXS curves also present an interference function under the influence of negatively charged porphyrins in HPS micelles, probably reflecting the same drug location at the inner HPS micellar interface.¹⁶ It should be noted, however, that both drug species, either positively charged as CPZ and TFP¹⁵ or negatively charged as anionic porphyrins,¹⁶ lead to a reduction of the overall size of HPS micelle, without affecting its spheroidal form.

On the other hand, the micellar growth accompanied by shape transformation from prolate ellipsoid to cylinder promoted by the presence of TFP and CPZ into LPC micelles parallels the effects previously observed upon incorporation of both phenothiazines to anionic sodium dodecyl sulfate micelles.^{14,15} What is remarkable is that the cationic drug promotes a surface charge screening in SDS micelles, whereas it induces a non-null surface charge density in zwitterionic LPC micelles.

Acknowledgment. The authors are indebted to FAPESP and CNPq Brazilian agencies for partial financial support. The support of the staff of the LNLS SAXS beamline is also greatly appreciated. L.R.S.B. is a recipient of Ph.D. CAPES fellowship. R.I. and M.T. are also grateful to CNPq for research grants. P.S.S. and P.H.M. are recipients of Ph.D. fellowships from FAPESP.

References and Notes

- (1) Parkanyi, C.; Boniface, C.; Aaron, J. J.; Maafi, M. *Spectrochim. Acta* **1993**, *12*, 1715–1720.
- (2) Ford, J. M.; Hait, W. N. *Pharmacol. Rev.* **1990**, *42*, 155–199.
- (3) Fowler, G. J. S.; Rees, R. C.; Devonshire, R. *Photochem. Photobiol.* **1990**, *52*, 489–494.
- (4) Ramu, A.; Ramu, N. *Cancer Chemother. Pharmacol.* **1992**, *30*, 165–173.
- (5) Luxnat, M.; Galla, H. J. *Biochim. Biophys. Acta* **1986**, *856*, 274–284.
- (6) Lieber, M. R.; Lange, Y.; Weinstein, R. S.; Steck, T. L. *J. Biol. Chem.* **1984**, *259*, 9225–9234.
- (7) Rosso, J.; Zachovskii, A.; Devaux, P. F. *Biochim. Biophys. Acta* **1988**, *942*, 271–279.
- (8) Suwalsky, M.; Gimenez, L.; Saenger, V.; Neira, F. Z. *Naturforsch.* **1988**, *43c*, 742–748.
- (9) Anteneodo, C.; Bish, P. M.; Ferreira Marques, J. *Eur. Biophys. J.* **1995**, *23*(6), 447–452.

- (10) Wajnberg, E.; Tabak, M.; Nussenzveig, P. A.; Lopes, C. M. B.; Louro, S. R. W. *Biochim. Biophys. Acta* **1988**, *944*, 185–190.
- (11) Attwood, D. *Adv. Colloid Interface Sci.* **1995**, *55*, 271–303.
- (12) Caetano, W.; Tabak, M. *Spectrochim. Acta* **1999**, *55A*, 2513–2528.
- (13) Caetano, W.; Tabak, M. *J. Colloid Int. Sci.* **2000**, *225*, 69–81.
- (14) Caetano, W.; Gelamo, E. L.; Tabak, M.; Itri, R. *J. Colloid Int. Sci.* **2002**, *248*, 149–157.
- (15) Caetano, W.; Barbosa, L. R. S.; Itri, R.; Tabak, M. *J. Colloid Int. Sci.* **2003**, *260*, 414–422.
- (16) Gandini, S. C. M.; Itri, R.; Neto, D. S.; Tabak, M. *J. Phys. Chem. B* **2005**, *109*, 22264–22272.
- (17) Klotarchyck, M.; Chen, S. H. *J. Chem. Phys.* **1983**, *79*, 2461–2469.
- (18) Itri, R.; Amaral, L. Q. *Phys. Rev. E* **1993**, *47*, 2551–2557.
- (19) Hayter, J. B.; Penfold, J. *Mol. Phys.* **1981**, *42*, 109–118.
- (20) Hansen, J. P.; Hayter, J. B. *Mol. Phys.* **1982**, *46*, 651–663.
- (21) Marignan, J.; Basseraud, P.; Delord, P. *J. Phys. Chem.* **1986**, *90*, 645–652.
- (22) Stewart, J. J. P. *J. Comput. Chem.* **1989**, *10*, 209–220.
- (23) Huibers, P. D. T. *Langmuir* **1999**, *15*, 7546–7550.
- (24) Motamedi, M.; Bathaie, S. Z.; Hemmateenejad, B.; Adjlou, D. *J. Mol. Struct. (THEOCHEM)* **2004**, *678*, 163–168.
- (25) Tanford, C. J. *Phys. Chem.* **1972**, *76*, 3020–3024.
- (26) Teixeira, C. V.; Itri, R.; Casallanovo, F.; Schreier, S. *Biochim. Biophys. Acta* **2001**, *1510*, 93–105.
- (27) Israelachvili, J. N.; Mitchell, D. J.; Ninham, B. W. *J. Chem. Soc., Faraday Trans. 2* **1976**, *72*, 1525–1568.
- (28) Akutsu, H.; Nagamori, T. *Biochemistry* **1991**, *30*, 4510–4516.
- (29) Wiener, M. C.; White, S. H. *Biophys. J.* **1992**, *61*, 434–447.
- (30) Forrest, B. J.; Linehan, P. T. P.; Mattai, J. *Biochemistry* **1984**, *23*, 2288–2293.